REAL-WORLD CONSIDERATIONS FOR CROSSED-POLARIZED UNDULATOR RADIATION CONVERSION*

W.M. Fawley†, E. Allaria, and E. Ferrari, Sincrotrone Trieste S.C.p.A., Trieste, Italy

Abstract

Cross-polarized (X-POL) configurations are a means to produce circularly-polarized radiation output from purely planar-polarized undulators. Recent polarization results from both the FERMI FEL-1 [1] at XUV wavelengths and Shanghai DUV-FEL [2] at visible wavelengths have confirmed that such configurations do work for single pass FELs. However, analysis of both FERMI and SINAP results indicate that the quantitative degree of planar to circular conversion can be significantly affected by several experimental details. Full conversion requires not only equal intensity of the two cross-polarized beams but also perfect overlap in space and time of their far-field amplitude and phase patterns. From simple theoretical analysis we examine a number of possible factors that can degrade the net linear to circular conversion efficiency. In addition to the previous suggestions by Ferrari *et al.* of problems with unbalanced powers and transverse phase variation arising from different effective emission z locations for the two cross-polarized radiation pulses, we also consider separate degradation effects of imperfect downstream overlap of the two linearly-polarized beams arising from different emission tilt angles and mode sizes. We also discuss optimizing the conversion efficiency by aperturing the radiation pulses downstream of the undulators.

INTRODUCTION

In addition to such attractive properties such as wavelength tunability, ultrashort and ultrabright output radiation, and multiple pulse production, free-electron lasers (FELs) with the proper undulator configurations can also produce variable polarization pulses. Because in many facilities linearly-polarized undulators have been favored due to their lower cost and often lower error content in comparison with variable-polarization designs such as the APPLE [3] and DELTA designs [4], the cross-polarized (X-POL) configuration has been suggested [5] as a relatively straight-forward means to produce output radiation with a high degree of circular polarization from purely linearly-polarized undulators. The X-POL arrangement has been studied for FEL amplifiers both theoretically [6, 7] and experimentally in the optical wavelength regime with circular-polarization degree 80% or greater [2].

Recently, experiments in October 2013 [1, 8] and more recently in February 2015 at the seeded FERMI FEL-1 facility [9] have shown the X-POL idea works reasonably well at wavelengths down to 26 nm. However, the 2013 results showed a global, maximum circular degree of polarization $P_{CIR} \leq 0.5$, suggesting that a careful tuning of the overall FEL system can be crucial for proper X-POL optimization. Indeed, the more recent X-POL results of February 2015 that included a careful optimization of the FEL using an online polarization diagnostic have shown significant improvement with a maximum $P_{CIR} \geq 0.8$. For the 2013 results, Ferrari *et al.* [8] suggested that an angular variation in far-field transverse eikonal phase between the horizontal- and vertically-polarized radiation due to different longitudinal source points in the undulator underlaid much of poor X-POL conversion. However, there are other possible degradation effects such as power imbalance of the two polarized fields and also imperfect spatial overlap arising from different emission tilt angles and mode sizes.

In the remainder of this paper we discuss these degradation issues and also the experimental procedures by which we believed we strongly improved the X-POL conversion efficiency as shown by the 2015 results.

THEORETICAL ANALYSIS

Inasmuch we are interested in the degree of circular polarization at a measurement point produced by spatial and temporal overlap of linearly-polarized sources the radiation properties are best described by the linear polarization basis for the Stokes parameters (see, *e.g.*, Eq. 7.27 of Jackson [10]):

$$S_0 \equiv a_H^2 + a_V^2 \qquad S_2 \equiv 2a_H\, a_V\, \cos\phi_{HV}$$
$$S_1 \equiv a_H^2 - a_V^2 \qquad S_3 \equiv 2a_H\, a_V\, \sin\phi_{HV} \qquad (1)$$

where a_H and a_V are the *local* field amplitudes of the two polarized beams, and $\phi_{HV} \equiv \varphi_H - \varphi_V$ is the difference of their eikonal phases. S_1 is the local, linearly-polarized signal lying in the horizontal/vertical plane while S_2 gives the strength of the signal component that is linearly-polarized in the skew planes at 45°/135°. Finally, S_3 measures the strength of the component with perfect circular polarization. The local value of the linear degree of polarization (the quantity that is actually measured in the FERMI studies discussed in the next section) $P_{LIN} = \sqrt{S_1^2 + S_2^2}/S_0$. The area integral of S_0 is proportional to the total power P_{TOT} of the two polarized beams while that of S_1 directly scales as $P_H - P_V$. The area integrals of S_2 and S_3 depend upon the details of their spatial overlap and relative phase at the measurement point. For the remainder of this discussion, we presume that the two sources are time-steady, monochromatic, exactly orthogonal, and define the horizontal and vertical planes.

Because the polarization measurements (see §III) are made in a "global" sense (here global refers to the total area

* This work was funded by the FERMI project of Elettra- Sincrotrone Trieste, supported in part by the Italian Ministry of University and Research under grants FIRB-RBAP045JF2 and FIRB-RBAP06AWK3
† william.fawley@elettra.eu

ISBN 978-3-95450-134-2

measured by the polarization detector), it becomes necessary to consider how local values of the Stokes parameters contribute to the global value. Clearly if the global value $\langle\langle S_1\rangle\rangle$ is non-zero, there must be residual linear polarization for all values of the relative phases ϕ_{HV} of the two beams and thus $P_{CIR} < 1$. However, it is also true that even if globally $\langle\langle S_1\rangle\rangle = 0$ but at local positions $S_1 \neq 0$, then both at those positions locally and more importantly *globally* $P_{CIR} < 1$. Such a situation can occur if for example the overall powers in the two linearly-polarized beams are exactly equal but either their mode shapes or sizes are different or, alternatively, if there is a transverse tilt between the two beams.

Similar phenomena are true for the S_2 and S_3 components where local values of $|S_2|$ might be large but the global value of $|\langle\langle S_2\rangle\rangle|$ can be zero. Unlike the S_1 parameter which by definition is insensitive to the relative phase ϕ_{HV}, both the local and, more importantly, global values of S_2 and S_3 depend upon this phase. For the FERMI X-POL experiments, the orthogonally-polarized sources originate in two different sets of undulators and ϕ_{HV} is varied by changing phase shifter strengths in the break sections. If we now make the *ansatz* that the temporal pulse shapes, radiated emission strength and transverse mode patterns of the two polarized beams are completely insensitive to variation of ϕ_{HV}, then if $\langle\langle S_2\rangle\rangle$ is non-zero for some given ϕ_{HV}, it must be *exactly* zero at some angle ϕ^0_{HV} in the interval $[\phi_{HV}, \phi_{HV} + \pi]$. At the two specific angles ϕ^0_{HV} and $\phi^0_{HV} + \pi$, we have must have the global minimum value of $P_{LIN} = |\langle\langle S_1\rangle\rangle| \,/\, \langle\langle S_0\rangle\rangle$ given our *ansatz* that neither locally nor globally S_0 or S_1 depend upon ϕ_{HV}.

Defining $x \equiv \min P_{LIN} = |P_H - P_V|/P_{TOT}$, one sees that $P_H = 0.5\,(1 + x)\,P_{TOT}$ and $P_V = 0.5\,(1 - x)\,P_{TOT}$, presuming $P_H \geq P_V$. If the two beams exactly overlap at the detector with the same profile, then the maximum possible circular polarization is $\sqrt{1 - x^2}$. For example, if $\min P_{LIN} = 0.5$, then 75% of the total power is in one of the two linear polarizations while only 25% is in the other; $\max P_{CIR} = 0.866$ presuming both perfect spatial overlap and constant eikonal phase difference between the two beams.

Measure of the linear polarization angle $\psi = 0.5 \tan^{-1} S_2/S_1$ while globally varying the phase shift between the two orthogonal sources also gives an indication of the downstream spatial and phase overlap properties. For perfect overlap and power balance, $\psi = \pm 45°$ and swings instantly at $\phi^0_{HV}, \phi^0_{HV} + \pi$ from one value to the other. For unbalanced powers but identical intensity and eikonal phase profiles,

$$\max|\psi| = 0.5\,\tan^{-1}\frac{0.5\sqrt{1 - x^2}}{x} \tag{2}$$

with the maxima in $|\psi|$ and $|d\psi/d\,\phi_{HV}|$ occurring in ϕ_{HV} at the locations of the maxima and minima of P_{LIN}, respectively. For $x = 0.5$, $\max\psi = 18.4°$ while for $x = 0.25$ the corresponding value is 31.3°. As we discuss in the next section, the behavior of both P_{LIN} and ψ as one scans in ϕ_{HV} can give an indication of the uniformity of the spatial overlap and relative eikonal phase variation of the two polarized beams.

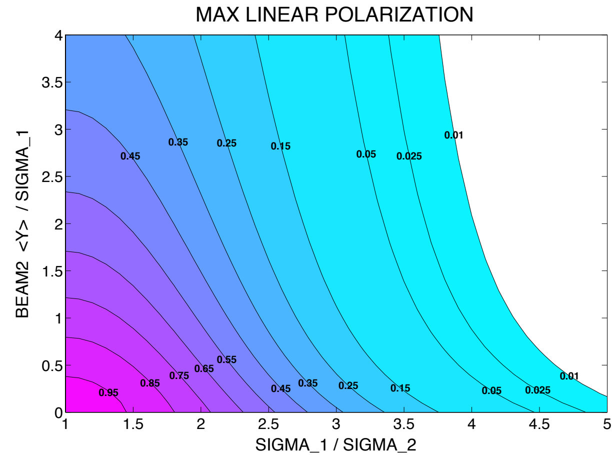

Figure 1: Contours mapping the maximum possible degree of linear polarization for two cross-polarized, gaussian profile beams with varying ratio of RMS radius σ_1/σ_2 and transverse offset of beam #2 from beam #1 in units of σ_1. There is perfect power balance and constant eikonal phase difference between the two beams.

In the case of perfect power balance (*i.e.*, $P_{LIN} = 0$ and $x = 0$), the maximum degree of linear polarization as one sweeps in over a full wavelength in phase shift between the two cross-polarized sources gives an indication of the uniformity of both the spatial overlap in intensity and eikonal phase difference of the two beams at the detector. In Figure 1 we plot the maximum degree of linear polarization for two equal power, cross-polarized sources in which the ratio σ_1/σ_2 of their downstream radii varies from 1 to 5 and for which the smaller beam's transverse offset $|\bar{y}|$ varies from 0 to 4 times the larger beam's electric field radius. Here we have presumed Gaussian profiles and a constant eikonal phase difference. One sees that for $\sigma_1/\sigma_2 \leq 1.5$ and $|\bar{y}|/\sigma_2 \leq 0.5$, one can still achieve greater than 85% linear polarization. Experimentally, such large values are quite obvious on downstream diagnostic screens and we believe in general that problems with maximum achievable polarization being significantly less than 0.9 are most likely due to a varying eikonal phase difference and/or different mode contents between the two beams.

FERMI EXPERIMENTAL RESULTS

The FERMI X-POL data of interest were taken with an electron time-of-flight (e-TOF) polarimeter developed at DESY and installed at FERMI under a collaborative effort (see [11–13] for more detail). On a shot-by-shot basis, this instrument measures at 16 individual stations equispaced in azimuthal angle θ the photoelectron signals produced by FEL radiation photoionization of He gas. The degree of *linear* polarization P_{LIN} and its angle ψ is then determined

ISBN 978-3-95450-134-2

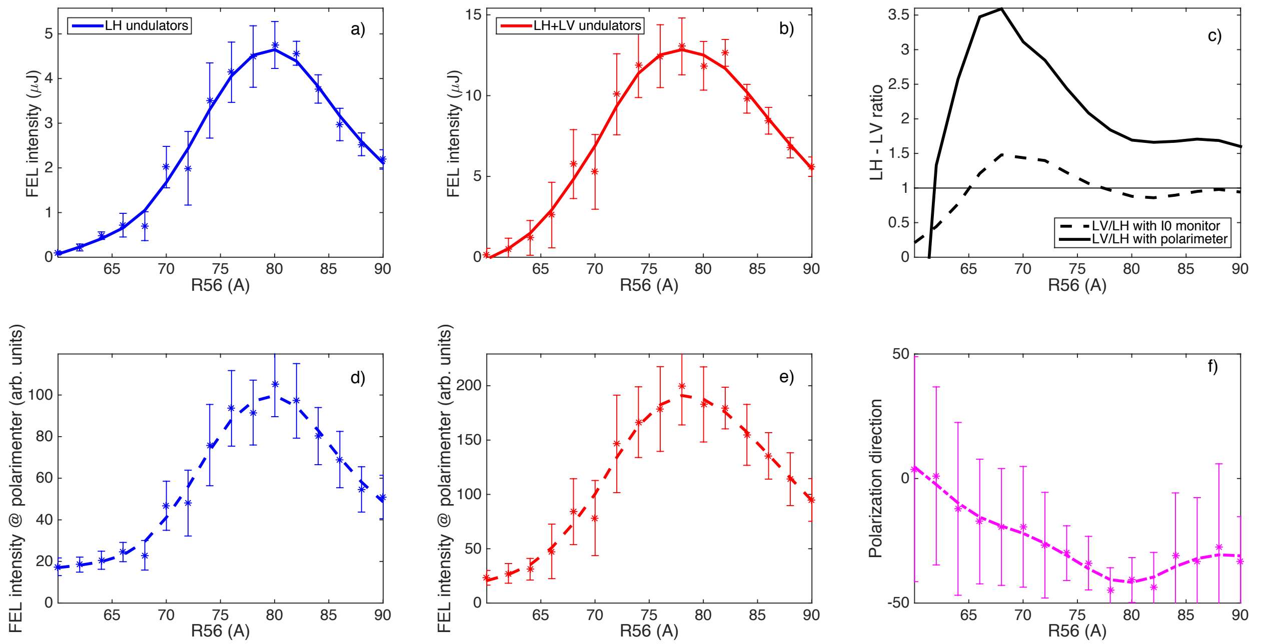

Figure 2: Variation of the output radiation power and its downstream degree of linear polarization via changing the FERMI FEL-1 post-modulator chicane current strength. This data was taken in February 2015. The panels labels a) and d) on the left display I0 and polarimeter power measurements, respectively, when only the upstream LH-polarized undulators were closed to FEL resonance. The center panels b) and e) refer to the measurements with all the LH- and LV-polarized undulators being closed. To the the right, panel c) shows the extacted power balance between the two polarizations (dashed line: I0 monitor data; solid line: polarimeter data) while panel f) indicates the measured polarization angle ψ. All error bars are the nominal RMS estimates.

from the signal data by using the theoretical relation

$$P(\theta) = 1 + \frac{1}{2}\{1 + 3\,P_{LIN}\ \cos[2(\theta - \psi)]\} \quad . \qquad (3)$$

In the process of optimizing an FEL for a cross-polarized configuration, it is critical to control the electron beam size and trajectory in the undulators. Moreover, the FEL needs to be controlled in a way that the emissions generated in the two groups of undulators have the same downstream properties. Since in the FERMI FEL-1 the field grows exponentially with z, balancing the power generated by each set of cross-polarized undulators can be difficult for the standard X-POL configuration where first a long undulator is used for one polarization, thus allowing the bunching and field to build up, followed by a second, much shorter undulator that produces the orthogonally-polarized radiation beam. Typically, there is little increase of bunching in the second undulator region and the second radiation beam is dominated by coherent spontaneous emission of a prebunched e-beam. In the case of an externally-seeded FEL such as FERMI, we found that power balance between the two beams is best achieved by manipulating the seeding and post-modulator chicane strength parameters. Importantly, we found in a recent set of experiments done in February 2015 that the best way to optimize matching between the two polarized radiation beams is to measure separately the FEL power of the two orthogonal sources at the downstream point where polarization control is actually wanted, or, alternatively, to examine the degree of the linear polarization of the combined fields.

Figure 2 reports an example of using an output intensity scan as a function of FERMI FEL-1's dispersive section strength as a means to balance the relative power between the two polarized sources. As one can see in Fig. 2a,b, according to measurements of the FEL power with the I0 gas-ionization monitor alone (whose position is quite close to the FEL source), it apparently is not possible in the present condition to get balanced emission between linear horizontal and linear vertical fields. Here we assumed that the measured output power from the two polarized beams will add linearly in the diagnostic; thus power balance would require twice the power in panel b) at a given dispersion strength relative to that in panel a). Considering only I0 measurements would then lead one to choose to a very different undulator configuration with respect to the one used here (*i.e.*, 4 undulators polarized LH and 2 LV). However if one use the FEL energy measurements from the polarimeter (*i.e.*, Fig. 2d,e), one sees a changing power balance ratio between the two polarizations as we change the chicane current and that an optimal, extracted ratio of 1.0 occurs at ≈ 78 A. Moreover, one can also measure directly the polarization properties while doing the optimization scan. Since in the case of a LH + LV cross-polarization, P_{LIN} depends on their relative phase ϕ_{HV} that is not known *a priori*, a better parameter for the optimization scans is the polarization angle ψ. As shown by Eq. 2 for power balance, this angle ideally does

ISBN 978-3-95450-134-2

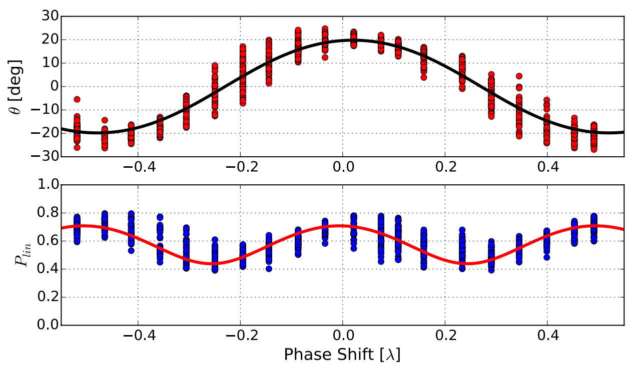

Figure 3: An example of the variation of linear polarization with phase shifter setting. In this case there is poor power balance and/or spatial overlap. The 32−nm data was taken in October 2013 on FERMI's FEL-1 with the DESY TOF polarimeter with the dots representing individual shots; typical statistical errors are of the order of 5%. The solid lines represent the predicted polarization dependence of two Gaussian profile sources with equal 100 μm waists separated by 3.7 m and whose field amplitudes differ by a factor of two.

not depend upon the relative phase and, for optimal power balance and overlap, should exhibit sudden changes from −45 to +45 degrees as one passes through the regime producing maximum circular polarization. Results reported in Fig. 2f show a clear trend for ψ with a local minimum at 43° for a dispersion section current ≈ 78 A. As would expected from perfect overlap theoretically, this corresponds to the dispersion section current value that also balances the power contributions from the LH- and LV-polarized undulator sections as seen in Figs. 2b,e.

These new results show the importance of an efficient, accurate, online diagnostic to determine the relative power between two cross-polarized sources. Indeed, if we had set the FEL based on the I0 detector power measurements, we would have obtained a condition where one of the two fields would be significantly stronger than the other. In retrospect, we believe such a situation occurred in our October 2013 X-POL measurements [8] which led to a reduced capability in polarization control as shown in Fig. 3. Indeed, it is important to note that the FEL power balance optimization done in the 2013 measurements used only the I0 monitor and we found that apparent balance required adopting a [4-LH + 1-LV] configuration rather than the far more successful [4-LH + 2-LV] configuration used more recently. For this situation, the power imbalance and the intensity and eikonal phase differnce effects of longitudinally-separated source points degrade both the degree of linear polarization and the maximum ψ achieved.

In February 2015 there were also a series of measurements in which the degree and angle of linear polarization was measured as a function of downstream, transverse position before which the combined beams were apertured upstream through an opening much smaller than their total size. Here we found that both the maximum and minimum polarization degree could be quite close to the perfect values of 1.0 and 0.0, again suggesting the smaller global values were due to relative intensity and eikonal phase variations. These results will be more fully reported elsewhere.

The authors are pleased to thank the FERMI operations crew and in particular the PADReS group for enabling the polarization observations of October 2013 and February 2015. We also gratefully acknowledge the FERMI collaboration with the DESY TOF polarimeter group and discussions with various team members.

REFERENCES

[1] E. Ferrari *et al.*, "Experimental Characterization of FEL Polarization Control with Cross Polarized Undulators", in *Proc. FEL'14*, Basel, Switzerland, Aug. 2014, paper THA02, pp. 644-648.

[2] H. Deng et al., *Phys. Rev. ST Accel. Beams* **17**, 020704 (2014).

[3] S. Sasaki, *Nucl. Instrum. Meth.* **A347**, 83-86 (1994).

[4] A.B. Temnykh, *Phys. Rev. ST Accel. Beams* **11**, 120702 (2008).

[5] K.-J. Kim, *Nucl. Instrum. Meth.* **A445**, 329 (2000).

[6] Y. Ding and Z. Huang, *Phys. Rev. ST Accel. Beams* **11**, 030702 (2008).

[7] Y. Li, B. Faatz, and J. Pflueger, *Nucl. Instrum. Meth.* **A613**, 163 (2010).

[8] E. Ferrari *et al.*, *Sci. Reports*, in press (2015).

[9] E. Allaria *et al.*, *Nat. Photonics* **6**, 699 (2012).

[10] J.D. Jackson, *Classical Electrodynamics*, 3rd Edition, Wiley, New York, p. 301 (1999).

[11] J. Viefhaus *et al.*, in *Coincidence Studies of Electron and Photon Impact Ionization*, ed. C.T. Whelan and H.R.J. Walters, *Physics of Atoms and Molecules*, Springer, pp. 145-153 (1997).

[12] J. Viefhaus, "An Online Diagnostic Unit for FEL Photon Parameter Determination and Optimization", presented at Proc. FEL'15, Daejeon, Korea, Aug. 2015, paper WED02, these proceedings.

[13] E. Allaria *et al.*, *Phys. Rev. X* **4**, 041040 (2014).

ISBN 978-3-95450-134-2